Revisiting the Noise Model of Stochastic Gradient Descent

Anonymous authors
Paper under double-blind review

Abstract

The stochastic gradient noise (SGN) is known as a significant factor in the success of stochastic gradient descent (SGD). Following the central limit theorem, SGN was initially modeled as Gaussian, and lately, it has been suggested that stochastic gradient noise is better characterized using $S\alpha S$ Lévy distribution. This claim was allegedly refuted and rebounded to the previously suggested Gaussian noise model. This paper presents solid and detailed empirical evidence that SGN is heavy-tailed and better depicted by the $S\alpha S$ distribution. Furthermore, we argue that different parameters in a deep neural network (DNN) hold distinct SGN characteristics throughout training. To more accurately approximate the dynamics of SGD near a local minimum, we construct a novel framework in $\mathbb{R}^N$, based on Lévy-driven stochastic differential equation (SDE), where one-dimensional Lévy processes model each parameter in the DNN. Next, we study the effect of learning rate decay (LRdecay) on the training process. We demonstrate theoretically and empirically that its main optimization advantage stems from the reduction of the SGN. Based on our analysis, we examine the mean escape time, trapping probability, and more properties of DNNs near local minima. Finally, we prove that the training process is more likely to exit from the basin in the direction of parameters with heavier tail SGN. We will share our code for reproducibility.

1 Introduction

The tremendous success of deep learning (Bengio, 2009; Hinton et al., 2012; LeCun et al., 2015) can be partly attributed to implicit properties of the optimization tools, in particular, the popular SGD (Robbins & Monro, 1951; Bottou, 1991) scheme. Despite its simplicity, i.e., being a noisy first-order optimization method, SGD empirically outperforms gradient descent (GD) and second-order methods. The stochastic gradient noise of stochastic gradient descent can improve the generalization of the model by escaping from sharp basins and settling in wide minima (Ziyin et al., 2021; Smith et al., 2020). SGD noise stems from the stochasticity in the mini-batch sampling operation, whose formation and amplitude are effected by the DNN architecture and data distribution. The main hurdle in improving deep learning is the lack of theory behind specific processes and modules frequently used; better understanding will help break current barriers in the field. Hence, a better understanding of SGD should be of the highest priority. Understanding the behavior of SGD optimization for non-convex cost functions, is an ongoing research (Chaudhari & Soatto, 2018; Zhou et al., 2019; Draxler et al., 2018; Nguyen & Hein, 2017; He et al., 2019b; Li et al., 2017; Smith et al., 2021; Ziyin et al., 2021; You et al., 2019). The problem of analyzing SGD noise has recently received much attention. Studies mainly examine the distribution and nature of the noise, with its ability to escape local minima and generalize better (Hu et al., 2017; He et al., 2019a; Wu et al., 2019; HaoChen et al., 2020; Zhou et al., 2019; Keskar et al., 2016).

SGD is based on an iterative update rule; the $k-th$ step of that iterative update rule is formulated as follows:

$$w_k = w_{k-1} - \frac{\eta}{B}\sum_{\ell\in\Omega_t}\nabla U^{(\ell)}(w_{k-1}) = w_{k-1} - \eta\nabla U(w_{k-1}) + \epsilon u_k, \tag{1}$$

where w denotes the weight (parameters) of the DNN, $\nabla U(w)$ is the gradient of the objective function, B is the batch size, $\Omega_k \subset \{1, .., D\}$ is the randomly selected mini-batch, thus $|\Omega_k| = B$, D is the number of data points in the dataset, u_k is the SGD noise and it is formulated as: $u_k = \nabla U(w_k) - \frac{1}{B}\sum_{\ell \in \Omega_k} \nabla U^{(\ell)}(w_k)$, i.e. the difference between the gradient produced by GD and SGD, finally $\epsilon = \eta^{\frac{\alpha-1}{\alpha}}$, and η is the learning rate.

As gradient flow is a popular apparatus to understand GD dynamics, continuous-time SDE is used to investigate SGD optimization process and examining the time evolution of the dynamic system in the continuous domain (Zhu et al., 2018; Meng et al., 2020; Xie et al., 2020; Chaudhari & Soatto, 2018; Hu et al., 2017; Sato & Nakagawa, 2014a).
Empiric experiments and their results produced a lively discussion on how SGN distributes, most of previous works (Zhu et al., 2018; Mandt et al., 2016; Wu et al., 2020; Ziyin et al., 2021): argue that the noise is Gaussian , i.e. $u_t \sim \mathcal{N}(0, \lambda(w_t))$, where $\lambda(w_t)$ is the noise covariance matrix and formulated as follows:

$$\lambda(W_t) = \frac{1}{B}\left[\frac{1}{D}\sum_{j=1}^{D} \nabla U^{(j)}(W_t)\nabla U^{(j)}(W_t)^T - \nabla U(W_t)\nabla U(W_t)^T\right]. \tag{2}$$

Recently, Zhu et al. (2018) showed the importance of modeling the SGN as an anisotropic noise to more accurately approximate SGD's dynamics. In Simsekli et al. (2019) the authors argue that SGN obeys $\mathcal{S}\alpha\mathcal{S}$ Lévy distribution, due to SGN's heavy-tailed nature. $\mathcal{S}\alpha\mathcal{S}$ Lévy process is described by a single parameter α_i also named "stability parameter" and holds unique properties, such as large discontinuous jumps. Therefore, Lévy-driven SDE does not depend on the height of the potential; on the contrary, it directly depends on the horizontal distance to the domain's boundary; this implies that the process can escape from narrow minima – no matter how deep they are and will stay longer in wide minima. In this work, we claim that the noise of different parameters in the DNN distributes differently and argue that it is crucial to incorporate this discrepancy into the SGN model. Hence, we model the training process as Lévy-driven stochastic differential equations (SDEs) in $\mathbb{R}^N$, where each parameter i distributes with a unique α_i; this formulation helps us investigate the properties and influence of each parameter on the training process.

Another critical aspect of NN optimization is the learning rate. Bengio (2012) argue that the learning rate is "the single most important hyper-parameter" in training DNNs; we yearn to understand what role does the LRdeacy has in SGN? Therefore, we examine the effect of the learning rate scheduler on the training process; considering two schedulers, the exponential scheduler $s_t = t^{\gamma-1}$ and the multi-step scheduler using p training phases with p different factors: $s_t = \gamma_p, \forall t \in (T_p, T_{p+1}]$, s.t $\gamma_p \in (0,1)$, the first is analysed for better theoretical reasoning, the last is a popular discrete scheduler used in modern DNNs training. We argue that decreasing the learning rate helps the optimization by attenuating the noise and not by reducing the step size; we brace the above claim using theoretical and experimental evidence.

Our contributions can be summarized as follows:

- This work empirically shows that the SGN of each parameter in a deep neural network is better characterized by $S\alpha S$ distribution.
- Our experiments strongly indicate that different parametric distributions characterize the noise of distinct parameters.
- We propose a novel dynamical system in $\mathbb{R}^N$ consisting of N one-dimensional Lévy processes with α_i-stable components and incorporates a learning rate scheduler to depict the training process better.
- Using our framework, we present an approximation of the mean escape time, the probability of escaping the local minima using a specific parameter, and more properties of the training process near local minima.
- We prove that parameters with lower α_i hold more probability to aid the training process to exit from local minima.
- We show that the effectiveness of the learning rate scheduler mainly evolves from noise attenuation and not step decaying.

2 Related Work

The study of stochastic dynamics of systems with small random perturbations is a well established field, first by modeling as Gaussian perturbations (Freidlin et al., 2012; Kramers, 1940), then replaced by Lévy noise with discontinuous trajectories (Imkeller & Pavlyukevich, 2006a; Imkeller et al., 2010; Imkeller & Pavlyukevich, 2008; Burghoff & Pavlyukevich, 2015). Modeling the noise as Lévy perturbations has attracted interest in the context of extreme events modeling, such as in climate (Ditlevsen, 1999), physics (Brockmann & Sokolov, 2002) and finance (Scalas et al., 2000).

Remark Let us remind that a Symmetric α stable distribution ($S\alpha S$ or Lévy $S\alpha S$) is a heavy-tailed distribution, parameterized by α - the stability parameter, smaller α leads to heavier tail (i.e. extreme events are more frequent and with more amplitude), and vice versa.

Modeling SGD using differential equations is a deep-rooted method, (Li et al., 2015) showed a framework of SDE approximation of SGD and focused on momentum and adaptive parameter tuning schemes and the dynamical properties of those stochastic algorithms. (Mandt & Blei, 2015) employed a similar procedure to derive an SDE approximation for the SGD to study issues such as choice of learning rates. (Li et al., 2015) showed that SGD can be approximated by an SDE in a first-order weak approximation. The early works in the field of studying SGD noise have approximated SGD by Langevin dynamic with isotropic diffusion coefficients (Sato & Nakagawa, 2014b; Raginsky et al., 2017; Zhang et al., 2017), later more accurate modeling suggested (Mandt et al., 2017; Zhu et al., 2018) using an anisotropic noise covariance matrix. Lately, it has been argued (Simsekli et al., 2019) that SGN is better characterized by $S\alpha S$ noise, presenting experimental and theoretical justifications. This model was allegedly refuted by (Xie et al., 2020), claiming that the experiments performed by (Simsekli et al., 2019) are inaccurate since the noise calculation was done across parameters and not across mini-batches. Lévy driven SDEs Euler approximation literature is sparser than for the Brownian motion SDEs; however, it is still intensely investigated; for more details about the convergence of Euler approximation for Lévy discretization, see (Mikulevicius & Zhang, 2010; Protter et al., 1997; Burghoff & Pavlyukevich, 2015).

Learning rate decay is an essential technique in training DNNs, investigated first for gradient descent (GD) by (LeCun et al., 1998). Kleinberg et al. (2018) showed that SGD is equivalent to the convolution of the loss surface, with the learning rate serving as the conceptual kernel size of the convolution. Hence spurious local minima can be smoothed out; thus, the decay of the learning rate later helps the network converge around the local minimum. You et al. (2019) suggested that learning rate decay improves the ability to learn complex separation patterns.

3 Framework and Main Results

In our analysis, we consider a DNN with $\bar{\mathbf{L}}$ layers and a total of N weights, the domain $\mathcal{G}$ is the local environment of a minimum, in this environment, the potential $U(W_t)$ is assumed $\mu-$strongly convex and C-*smooth* in $\mathcal{G}$ (see Appendix B.2 to better understand this assumption). Our framework considers an N-dimensional dynamic system, which represents the update rule of SGD as a Lévy-driven stochastic differential equation. In contrast to previous works (Zhou et al., 2020; Simsekli et al., 2019), our framework does not assume that SGN distributes the same for every parameter in the DNN. Thus, the SGN of each parameter is characterized by a different α. The governing SDE that depicts the SGDs dynamic inside the domain $\mathcal{G}$ is as follows:

$$W_t = w - \int_0^t \nabla U(W_p)\, dp + \sum_{l=1}^{N} s_t^{\frac{\alpha_l - 1}{\alpha_l}} \epsilon \mathbf{1}^T \lambda_l(t) r_l L_t^l, \tag{3}$$

where W_t is the process that depicts the evolution of DNN weights while training, $L_t^l \in \mathbb{R}$ is a mean-zero $S\alpha S$ Lévy processes with a stable parameter α_l. $\lambda_l(t) \in \mathbb{R}^N$ is the l-th row of the noise covariance matrix, $\mathbf{1} \in \mathbb{R}^N$ is a vector of ones and its purpose is to sum the l-th row of the noise covariance matrix. $r_l \in \mathbb{R}^N$ is a unit vector and we demand $|\langle r_i, r_j \rangle| \neq 1$, for $i \neq j$, we will use r_i as a one hot vector although it is not necessary. s_t will describe the learning rate scheduler, and w are the initial weights.

Remark L^l can be decompose into a small jump part ξ^l_t, and an independent part with large jumps ψ^l_t, i.e $L_l = \xi^l_t + \psi^l_t$, more information on $S\alpha S$ process is in A.2.

Let $\sigma_{\mathcal{G}} = \inf\{t \geq 0 : W_t \notin \mathcal{G}\}$ depict the first exit time from $\mathcal{G}$. τ^l_k denotes the time of the k-th large jump of parameter l driven by ψ^l process, where we define $\tau_0 = 0$. The interval between large jumps is denoted as: $S^l_k = \tau^l_k - \tau^l_{k-1}$ and is exponentially distributed with mean $\beta_i(t)^{-1}$, while τ^l_k is gamma distributed $Gamma(k, \beta_l(t))$; $\beta_l(t)$ is the jump intensity and will be fully define in Sec 3.2. We will define the arrival time of the k-th jump of all parameters combined as τ^*_k, for $k \geq 1$ by

$$\tau^*_k \triangleq \bigwedge_{\tau^l_j > \tau^*_{k-1}} \tau^l_j, \tag{4}$$

following that $S^*_k = \tau^*_k - \tau^*_{k-1}$.

Notations In what follows, an upper subscript denotes the DNN's parameter index, while a lower subscript denotes time if t is written or the discrete jump index unless it is specifically mentioned otherwise.

Jump heights are notated as: $J^l_k = \psi^l_{\tau_k} - \psi^l_{\tau_k -}$. We will define α_ν as the average α parameter over the entire DNN; this will help us describe the global properties of our network.
Let us define a measure of horizontal distance from the boundary of the domain using d^+_i and d^-_i; more assumptions and more rigorous formulation of the assumptions can be found in Sec. G.
To better understand the dynamics inside the basin (between the large jumps), we will define two more processes.

The deterministic process denoted as Y_t, is affected by the drift alone, without any perturbations. This process starts within the domain and does not escape this domain as time proceeds. The drift forces this process towards the stable point W^* as $t \to \infty$, i.e., the local minimum of the basin; furthermore, the process converges to the stable point exponentially fast and is defined for $t > 0$, and $w \in \mathcal{G}$ by:

$$Y_t = w - \int_0^t \nabla U(Y_s)\, ds. \tag{5}$$

The following Lemma shows how fast Y_t converges to the local minima from any starting point w inside the domain.

Lemma 3.1. *$\forall w \in \mathcal{G}$, $\tilde{U} = U(w) - U(W^*)$, the process Y_t converges to the minimum W^* exponentially fast:*

$$\|Y_t - W^*\|^2 \leq \frac{2\tilde{U}}{\mu} e^{-2\mu t}. \tag{6}$$

See the proof Appendix D.6

The small jumps process Z_t composed from the deterministic process Y_t and a stochastic process with infinite small jumps denoted as ξ_t (see more details in A.2). Z_t describes the system's dynamic in the intervals between the large jumps, hence we add an index k, that describes the jump index. Due to strong Markov property, $\xi^l_{t+\tau} - \xi^l_\tau, t \geq 0$ is also a Lévy process with the same law as ξ^l. Hence, for $t \geq 0$ and $k \geq 0$:

$$\xi^l_{t,k} = \xi^l_{t+\tau_{k-1}} - \xi^l_{\tau_{k-1}}. \tag{7}$$

The full small jumps process for $\forall t \in [0, S_k]$ is defined as:

$$Z_{t,k} = w + \int_0^t \nabla U(y_s) ds + \sum_{l=1}^{N} s_t^{\frac{\alpha_l - 1}{\alpha_l}} \epsilon \mathbf{1}^T \lambda_l(t) r_l \xi^l_{t,k}. \tag{8}$$

In the following proposition, we estimate the deviation of the solutions of the SDE driven by the process of the small jumps $Z^l_{t,k}$ from the deterministic trajectory in the l-th axis:

Proposition 3.2. *Let* $T_\epsilon > 0$ *exponentially distributed with parameter* β_l *,* $\forall w \in \mathcal{G}$*,* $c > 0$ *and* $\bar{\theta}_l \triangleq -\rho(1-\alpha_l) + 2 - 2\theta_l$ *, s.t* $\theta_l \in (0, \frac{2-\alpha_l}{4})$*, and* $C_{\theta_l} > 0$*, s.t. the following holds:*

$$P\left(\sup_{t\in[0,T_\epsilon]} |Z^l_{t,k}(w) - Y^l_{t,k}(w)| \geq c\bar{\epsilon}^{\theta_l}\right) \leq C_{\theta_l}\bar{\epsilon}^{\bar{\theta}_l} \tag{9}$$

Let us remind that: $\bar{\epsilon}_l = s_t^{\frac{\alpha_l - 1}{\alpha_l}}\epsilon_l$. In plain words, proposition 3.2 describes the distance between the deterministic process and the process of small jumps, between the occurrences of the large jumps. It indicates that between the large jumps, the processes are close to each other with high probability. Proof appears in D.3.

Next, we would like to learn another property of the process of the small jumps $Z^l_{t,k}$, that will aid us in better understanding the noise covariance matrix, but first let us present some notations, $H()$ is the hessian of the objective function, $u_{d,l}$ is the l-th component of $\nabla U_d(W^*)$ where the input is batch number d, $h_{l,j}$ represent the i-th row and j-th column of $H(W^*)$, and $h_{d,l,j}$ is the component in the l-th row and j-th column of $H(W^*)$ where the input is batch number d. Using stochastic asymptotic expansion, we are able to approximate $Z^l_{t,k}$ using the deterministic process and a first-order approximation of $Z^l_{t,k}$.

Lemma 3.3. *For a general scheduler* s_t*, let* $\mu^i_\xi = 2t\left[\frac{\bar{\epsilon}^{-\rho(1-\alpha_l)}-1}{1-\alpha_l}\right]$*,* $\rho \in (0,1)$ *,*$\bar{\epsilon}_l = s_t^{\frac{\alpha_l-1}{\alpha_l}}\epsilon_l$*,* h_{ll} *the second derivative of the drift in the l-th direction,* $\forall w_l, w_j \in \mathcal{G}$*, starting point after a big jump at time* $\tau^*_k + p$ *where* $p \to 0$*, and* $A_{lj}(t) \triangleq \bar{\epsilon}_l w_j e^{-h_{jj}t}\mu^l_\xi(2t + \frac{1}{h_{ll}}(1 - e^{-h_{ll}t}))$*, for* $t \in [0, S^*_k)$ *the following fulfills:*

$$\mathbb{E}[Z^l_{t,k}Z^j_{t,k}] \approx w_l w_j e^{-(h_{ll}+h_{jj})t} + A_{jl}(t) + A_{lj}(t) \tag{10}$$

Lemma 3.3 depicts the dynamics between two parameters in the intervals between the large jumps; this will aid in expressing the covariance matrix more explicitly; please examine the complete derivation of this result in the Appendix D.4.

3.1 Noise covariance matrix

The covariance of the noise matrix holds a vital role in modeling the training process; in this subsection, we aim to achieve an expression of the noise covariance matrix based on the stochastic processes we presented in previous subsection. . Using stochastic Taylor expansion near the basin W^*, we can achieve the following approximation.

Proposition 3.4. *Let us define* $\tilde{u}_l = \sum_{j=1}^N \nabla u_l \nabla u_j$*,* $\tilde{h}_{l,m,p,j} := \frac{1}{B}\sum_{b=1}^B h_{b,l,m}h_{b,p,j}$*,* $h_{l,m,p,j} := h_{l,m}h_{p,j}$ *and* $\bar{h}_{l,m,p,j} := \tilde{h}_{l,m,p,j} - h_{l,m,p,j}$*, then for any* $t \in [0, S^*_k)$*, the sum of the l-th row of the covariance matrix:*

$$\mathbf{1}^T\lambda^k_l(W_t) \approx \frac{1}{D}\sum_{j=1}^N \bar{u}_{lj} + \sum_{j=1}^N\sum_{m=1}^N\sum_{p=1}^N \bar{h}_{l,m,p,j}(w_m w_p e^{-(h_{mm}+h_{pp})t} + A_{mp}(t) + A_{pm}(t)), \tag{11}$$

where $A_{mp}(t)$ and $A_{pm}(t)$ are defined in lemma 3.3, see proof in Appendix D.5.(Reminder:D is the number of data points in the dataset).

3.2 Jump Intensity

Let us denote $\beta_l(t)$ as the jump intensity of the compound Poisson process ξ_l, $\beta_l(t)$ define how high will the process jump and the frequency of the jumps, which are distributed according to the law $\beta_l(t)^{-1}\nu_\eta$, and the jump intensity is formulated as:

$$\beta_l(t) = \nu_{\eta_l}(\mathbb{R}) = \int_{\mathbb{R}/[-O,O]} \nu_l(dy) = \frac{2}{\alpha_i}s_t^{\rho(\alpha_l-1)}\epsilon_l^{\rho\alpha_l}, \tag{12}$$

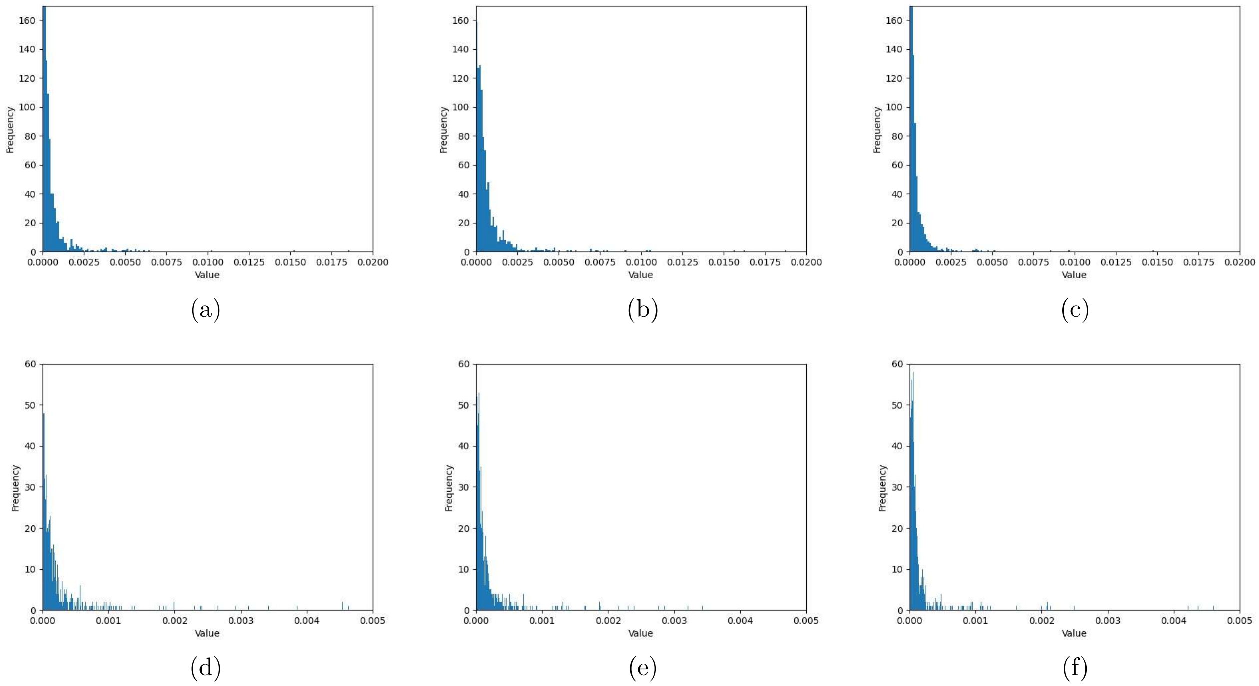

(a) (b) (c)

(d) (e) (f)

Figure 1: Histograms of the stochastic gradient noise for a single parameter. The top row shows the noise frequencies in ResNet18 for :(a) layer number 1, (b) layer number 2, and (c) layer number 3. The bottom row shows the noise frequencies in ResNet34 for: (d) layer number 1, (e) layer number 2, and (f) layer number 3..

Model	Gauss-SSE	$S\alpha S$-SSE	Gauss-Chi2	$S\alpha S$-Chi2
ResNet110	7.43	7.31	2.38	2.32
ResNet18	120.44	87.43	7.78	5.87
ResNet34	36.47	29.66	4.46	3.64
ResNet50	288.58	203.70	10.78	8.01

Table 1: The fitting error between SGN and $S\alpha S$/Gaussian distribution. Averaged over 100 randomly sampled parameters, four different CNNs trained on CIFAR100 with a batch size of 400. Two measures were used to evaluate the fitting error of each distribution, Sum of Squares Error (SSE) and Chi-Squares (Chi2). "Gauss" represents the Gaussian distribution.The results undoubtly shows that $S\alpha S$ better depicts SGN.

where the integration boundary is $O \triangleq \epsilon^{-\rho} s_t^{-\rho\frac{\alpha_l-1}{\alpha_l}}$, which is time-dependent, since the jump intensity is not stationary. The jump intensity is not stationary due to the learning rate scheduler, which decreases the size and frequency of the large jumps.

Let us notate $\beta_S(t) \triangleq \sum_{l=1}^{N} \beta_l(t)$, to ease the calculation we will assume that the time dependency: $\frac{\beta_l(t)}{\beta_S(t)} = \frac{\bar{\beta}_l}{\bar{\beta}_S} s^{\rho(\alpha_l - \alpha_\nu)}$. The probability of escaping the local minima in the first jump, in a single axis prospective, is denoted as:

$$P(s_t \epsilon \mathbf{1}^T \lambda_l(t) J_1^l \notin [d_l^-, d_l^+]) = \frac{m_l(t)\Phi_l s_t^{\alpha_l - 1}}{\beta_l(t)}, \tag{13}$$

where $m_l(t) = \frac{\mathbf{1}^T \lambda_l(t)_l^\alpha \epsilon_l^{\alpha_l}}{\alpha_l}$, and $\Phi_l = (-d_l^-)^{-\alpha_l} + (d_l^+)^{-\alpha_l}$.

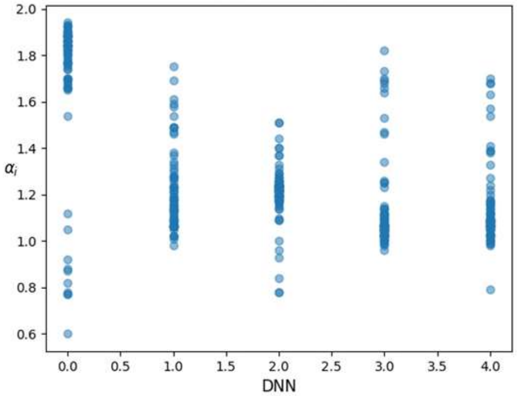

Figure 2: Each dot represents the distribution parameter α_i of a single weight in the DNN. Values on the x-axis represent five different DNNs, left to right: ResNet20/110/18/34/50 He et al. (2015); this plot confirms that distinct weights in a DNN lead to different noise distributions during training.

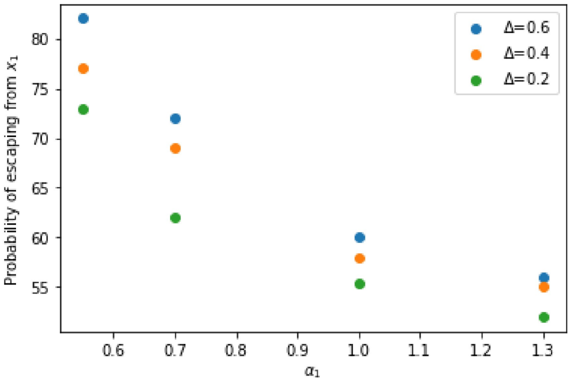

Figure 3: Four different values of α_1 and three values of Δ are selected, and the y-axis shows the probability of escaping from x_1, which is the axis with lower α. For example, the top-left most dot (blue) shows that when $\alpha_1 = 0.55$ and $\alpha_2 = 1.05$ the probability of the process to escape from axis x_1 is $\sim 82\%$.

4 Theorems

In the following section, we provide a theoretical analysis of SGD dynamics during the training of DNNs. Our analysis is based on two empirical pieces of evidence demonstrated in this work; the first is that SGN is indeed heavy-tailed. The second is that each parameter in the DNN's training process has a different stability parameter α drastically affects the noise properties.

Our work will assume that the training process can exit from the domain only at times that coincide with large jumps. Intuitively this assumption is based on a few realizations; first, in the domain $\mathcal{G}$, the deterministic process Y_t initialized in any point $w \in \mathcal{G}_\delta$ will converge to the local minima of the domain, second it converges to the minimum much faster then the time between the large jumps. Third, using lemma 3.1 we understand that the small jumps are less likely to aid the escape from the local minimum. Next, we will show evidence for the second realization mentioned above, the relaxation time T_R^l is the time for the deterministic process Y_t^l, starting from any arbitrary $w \in \mathcal{G}$, to reach an $\bar{\epsilon}_l^{\zeta}$-neighbourhood of the attractor. For some $C_1 > 0$, the relaxation time is

$$T_R^l = \max\left\{ \int_{d_l^-}^{-\bar{\epsilon}_l^{\zeta}} \frac{dy}{-U'(y)_l}, \int_{\bar{\epsilon}_l^{\zeta}}^{d_l^+} \frac{dy}{U'(y)_l} \right\} \leq C_1 |ln\bar{\epsilon}_l|. \tag{14}$$

Now, let us calculate the expectation of $S_k^* = \tau_k^* - \tau_{k-1}^*$, i.e. the interval between the large jumps:

$$\mathbb{E}[S_k^l] = \mathbb{E}[\tau_k^l - \tau_{k-1}^l] = \beta_l^{-1} = \frac{\alpha_l}{2} s_t^{-\rho\alpha_l} \epsilon^{-\rho\alpha_l}. \tag{15}$$

It is easy to notice that $\mathbb{E}[S_k^l] \gg T_R$, thus we can approximate that the process W_t is near the neighborhood of the basin, right before the large jumps. This means that it is highly improbable that two large jumps will occur before the training process returns to a neighborhood of the local minima. Using the knowledge above, we analyze the escaping time for exponential scheduler and for the multi-step scheduler, expanding our framework for more LRdecay schemes is straightforward. Let us define a constant that will be used for the remaining of the paper: $A_{l,\nu} \triangleq (1 - \bar{m}_\nu \bar{\beta}_\nu^{-1} \Phi_\nu)(1 - \bar{\beta}_l \bar{\beta}_S^{-1})$, for the next theorem we denote: $C_{l,\nu,p} \triangleq \frac{2+(\gamma-1)(\alpha_l - 1 + \rho(\alpha_l - \alpha_\nu))}{1+(\gamma-1)(\alpha_l - 1)}$, where $C_{l,\nu,p}$ depends on α_l, γ, and on the difference $\alpha_l - \alpha_\nu$. The following theorem describes the approximated mean transition time for the exponential scheduler:

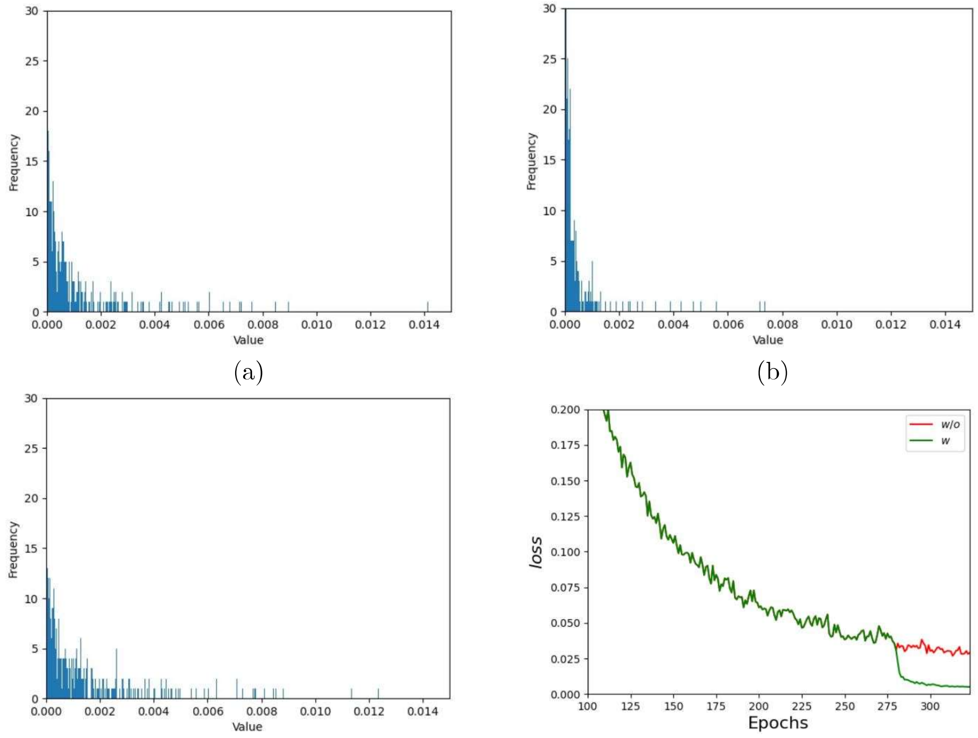

(a) (b)

(c) (d)

Figure 4: The stochastic gradient noise of a single parameter in ResNet110 He et al. (2015). (a) Before applying learning rate decay, at epoch 279. (b) After applying learning rate decay, at epoch 281. (c) Without learning rate decay, at epoch 281. (d) The training loss with and without learning rate decay applied at epoch 280.

Theorem 4.1. *Given $C_{l,\nu,p}$ and $A_{l,\nu}$, let s_t be an exponential scheduler $s_t = t^{\gamma-1}$,the mean transition time from the domain $\mathcal{G}$:*

$$\mathbb{E}[\sigma_{\mathcal{G}}] \leq \sum_{l=0}^{N} A_{l,\nu}^{-1} \frac{\beta_l(\bar{m}_l\Phi_l)^{1-C_{l,\nu,p}}}{\beta_S(1+(\gamma-1)(\alpha_l-1))}\Gamma\left(C_{l,\nu,p}\right)$$

Where Γ is the gamma function, $\bar{m}_l = \frac{\bar{\lambda}_l^{\alpha_l}\epsilon_l^{\alpha_l}}{\alpha_l}$ and $\bar{\beta}_l = \frac{2\bar{\lambda}_l^{\alpha_l}\epsilon_l^{\rho\alpha_l}}{\alpha_l}$ is the time independent jump intensity. For the full proof, see D.1. It can be easily observed from Thm. 4.1 that as γ decreases, i.e., faster learning rate decay, the mean transition time increases. Interestingly, when $\alpha_l \rightarrow 2$ (nearly Gaussian) and $\gamma \rightarrow 0$, the mean expectation time goes to infinity, which means that the training process is trapped inside the basin.

Corollary 4.2. *Using Thm. 4.1, if the cooling rate is negligible, i.e $\gamma \rightarrow 1$, the mean transition time:*

$$\mathbb{E}[\sigma_{\mathcal{G}}] \leq \sum_{l=0}^{N} A_{l,\nu}^{-1} \frac{1}{\beta_S 1^T \lambda_l \epsilon^{\alpha_l(1-\rho)}\Phi_l}. \tag{16}$$

There are a few observations from Corollary 4.2; first, we can see that there are two main global properties of the DNN inside the mean transition time expressions. The first, $A_{l,\nu}$ which describes the average α_ν of the network, the second is β_s which sums the jump intensities of all the parameters in the DNN. Second, it is intriguing to notice that modeling the perturbations as Lévy motion, SGD needs only polynomial time to exit the basin. This is in contrast to the case of Brownian motion, which requires an exponential time to transit to another basin.

Model	BS	Gauss-SSE	$S\alpha S$-SSE	Gauss-Chi2	$S\alpha S$-Chi2
Bert Base	8	2.15	0.71	1.41	0.42
Bert Base	32	0.37	0.18	0.19	0.11

Table 2: The fitting errors. The errors computed by averaging 120 randomly sampled parameters from BERT Devlin et al. (2018) model trained on the Cola dataset. Two measures were used to evaluate the fitting error of each distribution, Sum of Squares Error (SSE) and Chi-Squares (Chi2). Gauss represents the Gaussian distribution.

The framework presented in this work enables us to understand in which direction r_i the training process is more probable to exit the basin $\mathcal{G}$, i.e., which parameter is more liable to help the process escape; this is a crucial feature of our understanding in the training process and the role of individual parameters. The following theorems will be presented for the exponential scheduler but can be expanded for any scheduler.

Theorem 4.3. *Let s_t be an exponential scheduler $s_t = t^{\gamma-1}$, $C_l \triangleq \frac{(\gamma-1)(\alpha_l-1+\rho(2\alpha_l-\alpha_\nu-\alpha_l))+2}{(\gamma-1)(\alpha_l-1)+1}$, for $\delta \in (0, \delta_0)$, the probability of the training process to exit the basin through the l-th parameter is as follows:*

$$P(W_\sigma \in \Omega_i^+(\delta)) \leq \sum_{l=0}^{N} A_{l,\nu}^{-1} \frac{\bar{m}_l \Phi_l}{\bar{\beta}_l} (d_l^+)^{-\alpha_l} \frac{\beta_l^2 (\bar{m}_l \Phi_l)^{-C_l}}{\beta_S((\gamma-1)(\alpha_l-1)+1)} \Gamma\left(C_l\right). \tag{17}$$

Let us focus on the terms that describes the l-th parameter:

$$P(W_\sigma \in \Omega_l^+(\delta)) \leq \frac{\bar{m}_l}{\bar{\beta}_l} (d_l^+)^{-\alpha_l} \sum_{l=0}^{N} \tilde{C}_l, \tag{18}$$

where $\tilde{C}_l$ encapsulate all the terms that do not dependent on i. When considering SGN as Lévy noise, we can see that the training process needs only polynomial time to escape a basin. The following corollary helps us to assess the escaping ratio of two parameters.

Corollary 4.4. *The ratio of probabilities for exiting the local minima from two different DNN parameters is:*

$$\frac{P(W_\sigma \in \Omega_l^+(\delta))}{P(W_\sigma \in \Omega_j^+(\delta))} \leq \frac{1^T \lambda_l^{\alpha_l}}{1^T \lambda_j^{\alpha_j}} \epsilon^{(\alpha_l-\alpha_j)(1-\rho)} \frac{(d_l^+)^{-\alpha_l}}{(d_j^+)^{-\alpha_j}} \tag{19}$$

Let us remind the reader that (d_i^+) is a function of the horizontal distance from the domain's edge. Therefore, the first conclusion is that the higher (d_l^+) is, the probability of exiting from the l-th direction decreases. However, the dominant term is $\epsilon^{(\alpha_l-\alpha_j)(1-\rho)}$, combining both factors, it is clear that parameters with lower α will have more chance of being in the escape path. It can also be seen from the definition of β_l, that parameters with lower α jump earlier and contribute more significant jump intensities. We can conclude by writing:

$$\frac{P(W_\sigma \in \Omega_l^+(\delta))}{P(W_\sigma \in \Omega_j^+(\delta))} \propto \epsilon^{\Delta_{l,j}}, \tag{20}$$

where $\Delta_{l,j} = \alpha_l - \alpha_j$.

The rest of our theorems, are presented in the appendix.

5 Experiments

This section presents the core experimental results supporting our analysis; additional experiments can be found in Appendix. All the experiments were conducted using SGD without momentum and weight decay.

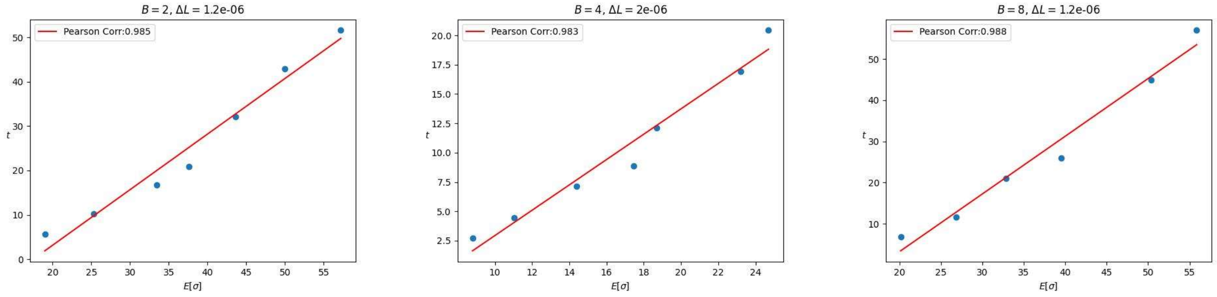

Figure 5: The x-axis represents the approximated upper bound of the escape time. The y-axis represents the number of iterations until exiting the basin; the strong correlation between the theory we presented and experiments is depicted visually by the red line and by Pearson correlation.

Stochastic gradient noise distribution First, we empirically show that SGN is better characterized using $S\alpha S$ Lévy distribution. Unlike previous works (Simsekli et al., 2019; Zhou et al., 2020; Xie et al., 2020) we will demonstrate not only visual experiments but also numeric results that will show the heavy-tailed nature of SGN.

We trained several CNNs on CINIC10 Darlow et al. (2018) and CIFAR100 Krizhevsky (2009) datasets, and a BERT base model on CoLA Warstadt et al. (2018) dataset until reaching convergence. We use several different batch sizes and different learning rates. Using the pre-trained weights, we sample 100 random parameters; for each parameter, we estimate the noise by computing the gradients of all of the mini-batches in the dataset without updating the weights. Then, we fitted the empiric stochastic gradient noise to multiple distributions; two metrics are used to evaluate the fitting process: Sum of square error (SSE) and Chi-Squares (Chi2) distance. Results for models trained on Cifar100 Krizhevsky (2009), are depicted in Tab. 1, results for models trained on CINIC10 Darlow et al. (2018) are shown in Tab. 3, the full tables can be seen in Sec. I.1.2. We examine the SGD noise of BERT model trained on CoLA Warstadt et al. (2018)dataset, the results are shown in Tab. 2. Visual examples for the heavy-tailed nature of SGN can be seen in Fig. 1, more visual results can be seen in Sec. I.1.1. Those evidences strength our claim of the heavy tailed nature of SGN, even for different DNN architectures (CNN and Transformer based models) and different input domains (text and images).
Remark The reader should notice that Xie et al. (2020) used random initialize weights to estimate the SGN histogram. We believe that assessing the noise based on randomly initialized weights does not correctly reflect the properties of SGD during the optimization process. In contrast, our experiments were performed during the training process (after the first few epochs).

Learning rate decay This paragraph aims to demonstrate that the LRdecay's effectiveness may be due to the attenuation of SGN. We show two experiments, first we trained ResNet110 He et al. (2015) on CIFAR100 Krizhevsky (2009), on epoch 280 the learning rate is decreased by a factor of 10. Fig. 4 shows that the learning rate decay results in a lower noise amplitude and less variance. In the second experiment, a ResNet20He et al. (2015) is trained in three different variations for 90 epochs; the first variation had LRdecay at epochs 30 and 60, the second had a batch-size increase at epochs 30 and 60, the third was trained with the same learning rate and batch size for the entire training process, the results show almost identical results on the first two cases, (i.e., LRdecay and batch increase) reaching a top-1 score of 66.7 and 66.4 on the validation set. In contrast, the third showed worse performances reaching a top-1 score of 53. Smith et al. (2017) performed similar experiments to show the similarity between decreasing the learning rate and increasing the batch size; however, their purpose was to suggest a method for improving training speed without degrading the results.

LRdecay decreases the step size and the noise amplitude; on the other hand, increasing the batch size only decreases the noise amplitude. Combining the results of the two experiments above, we may carefully deduce that the main effect of LRdecay is reducing the fluctuation in the gradient update phase and not decreasing the step size (step size is the movement of the deterministic process towards the minus of the gradient) . SGN amplitude reduction enables the training process to get easier localization in the current promising domain.

Different parameters hold different noise distributions? This experiment shows that different DNN parameters lead to distinct SGN during training. We randomly sampled 100 parameters from five different DNNs. Then, we calculated the SGN and estimated α_i for each parameter; Fig. 2 depicts the results for the five DNNs. It is clear that different parameters have noise that distributes differently during training. We can further notice that the variance is stretched on large segments of α_i values. This implies that building a framework that considers the DNN as one homogeneous system is insufficient; each parameter in the DNN has its own characteristic, and we should consider this when modeling the noise.

Escape Time. The following experiment validates Theorem. 4.1. We use a two-layer and a three-layer non-linear neural network, training on $2d$ synthetic data constructed from two Gaussian blobs. We first train the model until reaching a local minimum (see discussion Appendix B.1). Since we do not know the domain boundary of the current minimum, we measure the number of iterations until the training process passes a predefined loss delta (ΔL) from the current local minimum. Fig 5 shows the result of a two-layer neural network trained with different batch sizes, and the results are averaged upon 100 seeds. Additional experiments examining three layers NN, different data distributions, and different ΔL can be found in Appendix C.1.

Escaping Axis In this section, we demonstrate that the optimization process is more probable to escape from the axis with lower α_i. We use a 2D Ackleys function; the escape process starts at the global minimum $\vec{0}$. We apply Gradient Descent with added $S\alpha S$ noise ($S\alpha S(\alpha_{x_1})$,$S\alpha S(\alpha_{x_2})$), where $\alpha_1 = \alpha_2 - \Delta$. Once the optimization process passes some predefined radius, we check which axis is larger. Fig 3 shows how probable it is to exit from x_1 based on 1000 different seeds. This result implies that as the δ between the α_is increases, the axis with the smaller value of α has more probability of being the axis which the optimization process can escape through.

6 Conclusions

Our experiments undoubtedly show that the $S\alpha S$ better-characterized SGN visually and numerically. Furthermore, we showed that every parameter might evolve noise with distinct distribution parameter α. We also presented experiments that support the claim that the main feature of LR schedulers comes from reducing the fluctuations of the SGN. Based on the mentioned experiments, we constructed a framework in $\mathbb{R}^N$ consisting of N one-dimensional Lévy processes with α_i-stable components. This framework enables us to understand the nature of DNN training better using SGD, such as the escaping properties from different local minima, a learning rate scheduler, and other parameters' effects in the DNN. Finally, we showed that parameters in the DNN that hold noise that distributes with low α_i have a unique role in the training process, helping the training process escape local minima.

Limitations and Future Research The presented framework is valid once the training process is near a local minimum; how the training acts in other states, for example, at the beginning of the training, is not intended to be solved in this work. Further, how α evolves is still unclear and demands future research. Experimental limitations are essential to discuss; The SGD in this work does not include momentum, weight decay in order to be aligned with the theory.

Please notice that there are more theorems, lemmas, additional experiments, plots, and the complete proofs in the Appendix.

Broader Impact Statement

One of Deep learning main drawbacks is the lack of a fundamental theory, understanding this theory is critical for the advancement of the field. Surprisingly, the noise in SGD,is crucial in DNN optimization process, in this work we shed light on SGN distribution and effects on the training process, reveling a hand-breadth of it's mystery.

References

Herbert Amann. *Gewöhnliche differentialgleichungen*. Walter de Gruyter, 2011.

Vlad Bally and Denis Talay. The law of the euler scheme for stochastic differential equations: Ii. convergence rate of the density. 1996.

Yoshua Bengio. *Learning deep architectures for AI*. Now Publishers Inc, 2009.

Yoshua Bengio. Practical recommendations for gradient-based training of deep architectures. In *Neural networks: Tricks of the trade*, pp. 437–478. Springer, 2012.

Léon Bottou. Stochastic gradient learning in neural networks. *Proceedings of Neuro-Nımes*, 91(8):12, 1991.

Dirk Brockmann and IM Sokolov. Lévy flights in external force fields: from models to equations. *Chemical Physics*, 284(1-2):409–421, 2002.

Toralf Burghoff and Ilya Pavlyukevich. Spectral analysis for a discrete metastable system driven by lévy flights. *Journal of Statistical Physics*, 161(1):171–196, 2015.

Pratik Chaudhari and Stefano Soatto. Stochastic gradient descent performs variational inference, converges to limit cycles for deep networks. In *2018 Information Theory and Applications Workshop (ITA)*, pp. 1–10. IEEE, 2018.

Yunpeng Chen, Yannis Kalantidis, Jianshu Li, Shuicheng Yan, and Jiashi Feng. Multi-fiber networks for video recognition. In *Proceedings of the European Conference on Computer Vision (ECCV)*, September 2018.

Umut Şimşekli. Fractional Langevin Monte Carlo: Exploring Lévy Driven Stochastic Differential Equations for Markov Chain Monte Carlo. *arXiv e-prints*, art. arXiv:1706.03649, June 2017.

Luke N. Darlow, Elliot J. Crowley, Antreas Antoniou, and Amos J. Storkey. CINIC-10 is not ImageNet or CIFAR-10. *arXiv e-prints*, art. arXiv:1810.03505, October 2018.

Jacob Devlin, Ming-Wei Chang, Kenton Lee, and Kristina Toutanova. BERT: Pre-training of Deep Bidirectional Transformers for Language Understanding. *arXiv e-prints*, art. arXiv:1810.04805, October 2018.

Peter D Ditlevsen. Observation of α-stable noise induced millennial climate changes from an ice-core record. *Geophysical Research Letters*, 26(10):1441–1444, 1999.

Felix Draxler, Kambis Veschgini, Manfred Salmhofer, and Fred Hamprecht. Essentially no barriers in neural network energy landscape. In *International conference on machine learning*, pp. 1309–1318. PMLR, 2018.

Jinqiao Duan. *An introduction to stochastic dynamics*, volume 51. Cambridge University Press, 2015.

M.I. Freidlin, J. Szücs, and A.D. Wentzell. *Random Perturbations of Dynamical Systems*. Grundlehren der mathematischen Wissenschaften. Springer, 2012. ISBN 9783642258473. URL `http://books.google.de/books?id=p8LFMILAiMEC`.

Thomas Hakon Gronwall. Note on the derivatives with respect to a parameter of the solutions of a system of differential equations. *Annals of Mathematics*, pp. 292–296, 1919.

Jeff Z HaoChen, Colin Wei, Jason D Lee, and Tengyu Ma. Shape matters: Understanding the implicit bias of the noise covariance. *arXiv preprint arXiv:2006.08680*, 2020.

Fengxiang He, Tongliang Liu, and Dacheng Tao. Control batch size and learning rate to generalize well: Theoretical and empirical evidence. 2019a.

Haowei He, Gao Huang, and Yang Yuan. Asymmetric valleys: Beyond sharp and flat local minima. *arXiv preprint arXiv:1902.00744*, 2019b.

Kaiming He, Xiangyu Zhang, Shaoqing Ren, and Jian Sun. Deep Residual Learning for Image Recognition. *arXiv e-prints*, art. arXiv:1512.03385, December 2015.

Geoffrey Hinton, Li Deng, Dong Yu, George E Dahl, Abdel-rahman Mohamed, Navdeep Jaitly, Andrew Senior, Vincent Vanhoucke, Patrick Nguyen, Tara N Sainath, et al. Deep neural networks for acoustic modeling in speech recognition: The shared views of four research groups. *IEEE Signal processing magazine*, 29(6):82–97, 2012.

Wenqing Hu, Chris Junchi Li, Lei Li, and Jian-Guo Liu. On the diffusion approximation of nonconvex stochastic gradient descent. *arXiv e-prints*, art. arXiv:1705.07562, May 2017.

Peter Imkeller and Ilya Pavlyukevich. First exit times of sdes driven by stable lévy processes. *Stochastic Processes and their Applications*, 116(4):611–642, 2006a.

Peter Imkeller and Ilya Pavlyukevich. Lévy flights: transitions and meta-stability. *Journal of Physics A: Mathematical and General*, 39(15):L237, 2006b.

Peter Imkeller and Ilya Pavlyukevich. Metastable behaviour of small noise lévy-driven diffusions. *ESAIM: Probability and Statistics*, 12:412–437, 2008.

Peter Imkeller, Ilya Pavlyukevich, and Michael Stauch. First exit times of non-linear dynamical systems in d perturbed by multifractal lévy noise. *Journal of Statistical Physics*, 141(1):94–119, 2010.

Jean Jacod, Thomas G Kurtz, Sylvie Méléard, and Philip Protter. The approximate euler method for lévy driven stochastic differential equations. In *Annales de l'IHP Probabilités et statistiques*, volume 41, pp. 523–558, 2005.

Nitish Shirish Keskar, Dheevatsa Mudigere, Jorge Nocedal, Mikhail Smelyanskiy, and Ping Tak Peter Tang. On large-batch training for deep learning: Generalization gap and sharp minima. *arXiv preprint arXiv:1609.04836*, 2016.

Bobby Kleinberg, Yuanzhi Li, and Yang Yuan. An alternative view: When does sgd escape local minima? In *International Conference on Machine Learning*, pp. 2698–2707. PMLR, 2018.

Hendrik Anthony Kramers. Brownian motion in a field of force and the diffusion model of chemical reactions. *Physica*, 7(4):284–304, 1940.

Alex Krizhevsky. Learning multiple layers of features from tiny images. Technical report, 2009.

H. Kuehne, H. Jhuang, E. Garrote, T. Poggio, and T. Serre. HMDB: A large video database for human motion recognition. In *2011 Int. Conf. Comput. Vis.*, pp. 2556–2563. IEEE, nov 2011. ISBN 978-1-4577-1102-2. doi: 10.1109/ICCV.2011.6126543. URL `http://ieeexplore.ieee.org/document/6126543/`.

Yann LeCun, Yoshua Bengio, and Geoffrey Hinton. Deep learning. *nature*, 521(7553):436–444, 2015.

Yann A LeCun, Léon Bottou, Genevieve B Orr, and Klaus-Robert Müller. Efficient backprop. In *Neural networks: Tricks of the trade*, pp. 9–48. Springer, 1998.

Hao Li, Zheng Xu, Gavin Taylor, Christoph Studer, and Tom Goldstein. Visualizing the loss landscape of neural nets. *arXiv preprint arXiv:1712.09913*, 2017.

Qianxiao Li, Cheng Tai, and Weinan E. Stochastic modified equations and adaptive stochastic gradient algorithms. *arXiv e-prints*, art. arXiv:1511.06251, November 2015.

Qianxiao Li, Cheng Tai, and E Weinan. Dynamics of stochastic gradient algorithms. *ArXiv*, abs/1511.06251, 2015.

Stephan Mandt and David M. Blei. Continuous-time limit of stochastic gradient descent revisited. 2015.

Stephan Mandt, Matthew D. Hoffman, and David M. Blei. A Variational Analysis of Stochastic Gradient Algorithms. *arXiv e-prints*, art. arXiv:1602.02666, February 2016.

Stephan Mandt, Matthew D Hoffman, and David M Blei. Stochastic gradient descent as approximate bayesian inference. *arXiv preprint arXiv:1704.04289*, 2017.

Qi Meng, Shiqi Gong, Wei Chen, Zhi-Ming Ma, and Tie-Yan Liu. Dynamic of Stochastic Gradient Descent with State-Dependent Noise. *arXiv e-prints*, art. arXiv:2006.13719, June 2020.

Qi Meng, Shiqi Gong, Wei Chen, Zhi-Ming Ma, and Tie-Yan Liu. Dynamic of stochastic gradient descent with state-dependent noise. *arXiv preprint arXiv:2006.13719*, 2020.

R. Mikulevicius and C. Zhang. On the rate of convergence of weak Euler approximation for non-degenerate SDEs. *arXiv e-prints*, art. arXiv:1009.4728, September 2010.

Quynh Nguyen and Matthias Hein. The loss surface of deep and wide neural networks. In *International conference on machine learning*, pp. 2603–2612. PMLR, 2017.

Fabien Panloup. Recursive computation of the invariant measure of a stochastic differential equation driven by a Lévy process. *arXiv Mathematics e-prints*, art. math/0509712, September 2005.

Philip Protter, Denis Talay, et al. The euler scheme for lévy driven stochastic differential equations. *The Annals of Probability*, 25(1):393–423, 1997.

Maxim Raginsky, Alexander Rakhlin, and Matus Telgarsky. Non-convex learning via stochastic gradient langevin dynamics: a nonasymptotic analysis. In *Conference on Learning Theory*, pp. 1674–1703. PMLR, 2017.

Herbert Robbins and Sutton Monro. A stochastic approximation method. *The annals of mathematical statistics*, pp. 400–407, 1951.

Issei Sato and Hiroshi Nakagawa. Approximation analysis of stochastic gradient langevin dynamics by using fokker-planck equation and ito process. In Eric P. Xing and Tony Jebara (eds.), *Proceedings of the 31st International Conference on Machine Learning*, volume 32 of *Proceedings of Machine Learning Research*, pp. 982–990, Bejing, China, 22–24 Jun 2014a. PMLR. URL `http://proceedings.mlr.press/v32/satoa14.html`.

Issei Sato and Hiroshi Nakagawa. Approximation analysis of stochastic gradient langevin dynamics by using fokker-planck equation and ito process. In *International Conference on Machine Learning*, pp. 982–990. PMLR, 2014b.

Enrico Scalas, Rudolf Gorenflo, and Francesco Mainardi. Fractional calculus and continuous-time finance. *Physica A: Statistical Mechanics and its Applications*, 284(1-4):376–384, 2000.

Umut Simsekli, Levent Sagun, and Mert Gurbuzbalaban. A tail-index analysis of stochastic gradient noise in deep neural networks. In *International Conference on Machine Learning*, pp. 5827–5837. PMLR, 2019.

Samuel Smith, Erich Elsen, and Soham De. On the generalization benefit of noise in stochastic gradient descent. In *International Conference on Machine Learning*, pp. 9058–9067. PMLR, 2020.

Samuel L Smith, Pieter-Jan Kindermans, Chris Ying, and Quoc V Le. Don't decay the learning rate, increase the batch size. *arXiv preprint arXiv:1711.00489*, 2017.

Samuel L Smith, Benoit Dherin, David GT Barrett, and Soham De. On the origin of implicit regularization in stochastic gradient descent. *arXiv preprint arXiv:2101.12176*, 2021.

Alex Warstadt, Amanpreet Singh, and Samuel R Bowman. Neural network acceptability judgments. *arXiv preprint arXiv:1805.12471*, 2018.

Jingfeng Wu, Wenqing Hu, Haoyi Xiong, Jun Huan, and Zhanxing Zhu. The multiplicative noise in stochastic gradient descent: Data-dependent regularization, continuous and discrete approximation. *CoRR*, 2019.

Jingfeng Wu, Wenqing Hu, Haoyi Xiong, Jun Huan, Vladimir Braverman, and Zhanxing Zhu. On the noisy gradient descent that generalizes as sgd. In *International Conference on Machine Learning*, pp. 10367–10376. PMLR, 2020.

Zeke Xie, Issei Sato, and Masashi Sugiyama. A diffusion theory for deep learning dynamics: Stochastic gradient descent exponentially favors flat minima. *arXiv e-prints*, pp. arXiv–2002, 2020.

Kaichao You, Mingsheng Long, Jianmin Wang, and Michael I. Jordan. How Does Learning Rate Decay Help Modern Neural Networks? *arXiv e-prints*, art. arXiv:1908.01878, August 2019.

Yuchen Zhang, Percy Liang, and Moses Charikar. A hitting time analysis of stochastic gradient langevin dynamics. In *Conference on Learning Theory*, pp. 1980–2022. PMLR, 2017.

Mo Zhou, Tianyi Liu, Yan Li, Dachao Lin, Enlu Zhou, and Tuo Zhao. Toward understanding the importance of noise in training neural networks. In *International Conference on Machine Learning*, pp. 7594–7602. PMLR, 2019.

Pan Zhou, Jiashi Feng, Chao Ma, Caiming Xiong, Steven Hoi, et al. Towards theoretically understanding why sgd generalizes better than adam in deep learning. *arXiv preprint arXiv:2010.05627*, 2020.

Zhanxing Zhu, Jingfeng Wu, Bing Yu, Lei Wu, and Jinwen Ma. The Anisotropic Noise in Stochastic Gradient Descent: Its Behavior of Escaping from Sharp Minima and Regularization Effects. *arXiv e-prints*, art. arXiv:1803.00195, February 2018.

Liu Ziyin, Kangqiao Liu, Takashi Mori, and Masahito Ueda. On minibatch noise: Discrete-time sgd, overparametrization, and bayes. *arXiv preprint arXiv:2102.05375*, 2021.